Intersample Behavior Analysis of MIMO Multirate Feedforward Control depending on Selection of Input Multiplicities

Masahiro Mae * **Wataru Ohnishi** * **Hiroshi Fujimoto** *

* *The University of Tokyo 5-1-5, Kashiwanoha, Kashiwa, Chiba, 277-8561, Japan (e-mail: mmae@ieee.org, ohnishi@ieee.org, fujimoto@k.u-tokyo.ac.jp)*

Abstract: Perfect tracking control method using multirate feedforward control is a very effective control method in high-precision positioning systems since this method provides zero tracking error for a nominal plant at every reference sampling point theoretically. When we design a multirate feedforward controller for a multi-input multi-output system, it is known that several types of controllers can be designed depending on how to select input multiplicities. Although multirate feedforward controllers provide perfect tracking at every reference sampling point theoretically, intersample behavior is different. In this paper, we propose the stable state trajectory generation method and the guideline to design an optimal multi-input multi-output multirate feedforward controller considering the 2-norm of control input and improve the intersample behavior. The effectiveness of the proposed method is verified in the simulation.

Keywords: Feedforward control, Digital control, Multirate, Multi-input/multi-output systems, Inverse system

1. INTRODUCTION

Perfect tracking control (PTC) using multirate feedforward control is widely used for controlling precision positioning systems in industrial application fields such as manufacturing semiconductors and flat panels, and controlling a head of hard disk drives. Multirate feedforward control provides perfect tracking control [Fujimoto et al. (2001)]. The word "perfect tracking control" is defined as "the plant output perfectly tracks the desired trajectory with zero tracking error at every sampling point" [Tomizuka (1987)]. Perfect tracking cannot be achieved by a single-rate control scheme because of unstable zeros due to discretization of the plant using zero-order hold [Tomizuka (1987)]. Therefore, several studies are conducted for the approximated plant model inverse approaches in the single-rate control scheme such as nonminimum-phase zeros ignore (NPZI) method [Butterworth et al. (2012)], zero-phase-error tracking controller (ZPETC) method [Tomizuka (1987)] and zero-magnitude-error tracking controller (ZMETC) method [Wen and Potsaid (2004)]. Multirate feedforward control solves the problem of discretization unstable zeros and provides perfect tracking control [Fujimoto et al. (2001)].

Recently, many mechatronic systems are used in industrial applications and the precision positioning systems in these mechatronic systems are becoming multi-input multi-output (MIMO) systems to improve performance [Butler (2011)]. Because of coupling problems in each axis, a sufficient control performance cannot be expected for MIMO systems when the simple single-input single-output (SISO) controllers are designed for each axis, respectively. Therefore, to overcome coupling problems in MIMO systems, it is necessary to treat controlled systems as MIMO systems and design MIMO feedforward controllers. When the multirate feedforward controllers are designed for MIMO systems, several kinds of controllers can be designed depending on the selection of input multiplicities [Fujimoto (2000)]. All designed multirate feedforward controllers achieve perfect tracking control, however, intersample performances are different depending on the controller designs [Mae et al. (2018)]. Perfect tracking control is defined in the framework of a digital control system [Fujimoto et al. (2001)]. Therefore, there is no consideration of the tracking error between sampling points. For this reason, even if several kinds of multirate feedforward controllers for MIMO systems achieve perfect tracking on sample points, the optimal controller can be chosen from the view of the intersample behavior.

In this paper, we propose the state space representation using singular value decomposition which gathers continuous time invariant zeros into the part of the state trajectory generation. We solve the problem due to unstable invariant zeros of the controlled system in the state trajectory generation and improve the intersample behavior. We also propose the guideline how to choose input multiplicities to design the optimal MIMO multirate feedforward controller from viewpoint of the 2-norm of control input. When the 2-norm of control input is too large, it is not suitable for the mechatronic systems. We aim to make the 2-norm of control input smaller and the smaller control input also tend to the smaller tracking error between sampling points.

Conventionally, the intersample behavior is evaluated by simulation results, but, it costs much more time when many kinds of controllers can be designed. We propose

the guideline how to evaluate the 2-norm of control input and choose an optimal controller before the simulation. The effectiveness of the proposed method is verified in the simulation of the two-inertia motor bench system.

2. STATE TRAJECTORY GENERATION FOR MULTI-INPUT MULTI-OUTPUT SYSTEM

The proposed method of generating the state trajectory from the output trajectory in the MIMO system will be described below. Using a proposed state space representation, an intersample problem which is occurred by the continuous time unstable invariant zeros is solved in the part of a state trajectory generation. In this study, the plant is assumed to be an m-input m-output nth order plant, where $m < n$ and $\mathrm{rank}(\boldsymbol{B}) = m$.

2.1 Definition of multi-input multi-output system

The state equation and the output equation for an m-input m-output nth order plant are given by

$$\dot{\boldsymbol{x}}(t) = \boldsymbol{A}\boldsymbol{x}(t) + \boldsymbol{B}\boldsymbol{u}(t), \tag{1}$$
$$\boldsymbol{y}(t) = \boldsymbol{C}\boldsymbol{x}(t), \tag{2}$$

where the state variables are $\boldsymbol{x}(t) \in \mathbb{R}^{n\times 1}$, each input is $\boldsymbol{u}(t) \in \mathbb{R}^{m\times 1}$, each output is $\boldsymbol{y}(t) \in \mathbb{R}^{m\times 1}$, and the matrices are $\boldsymbol{A} \in \mathbb{R}^{n\times n}$, $\boldsymbol{B} \in \mathbb{R}^{n\times m}$, and $\boldsymbol{C} \in \mathbb{R}^{m\times n}$.

2.2 State space representation of MIMO system

Singular value decomposition of $\boldsymbol{B}$ matrix Singular value decomposition of the matrix $\boldsymbol{B}$ is given by

$$\boldsymbol{B} = \boldsymbol{U}\boldsymbol{\Sigma}\boldsymbol{V}^{\mathsf{H}}, \tag{3}$$

where $\boldsymbol{U} \in \mathbb{R}^{n\times n}$, $\boldsymbol{\Sigma} \in \mathbb{R}^{n\times m}$, $\boldsymbol{V} \in \mathbb{R}^{m\times m}$.

The elements of $\boldsymbol{\Sigma}$ are given by

$$\boldsymbol{\Sigma} = \begin{bmatrix} \boldsymbol{\Delta} \\ \boldsymbol{O} \end{bmatrix},$$
$$\boldsymbol{\Delta} = \mathrm{diag}(\sigma_i)\,(i = 1 \cdots m \in \mathbb{N}),$$

where $\sigma_i\,(i = 1, 2, \ldots, m \in \mathbb{N})$ are the singular values of the matrix $\boldsymbol{B}$.

Multiplying both sides of (3) by $\boldsymbol{U}^{\mathsf{H}}$ from the left yields

$$\boldsymbol{U}^{\mathsf{H}}\boldsymbol{B} = \boldsymbol{\Sigma}\boldsymbol{V}^{\mathsf{H}} = \begin{bmatrix} \boldsymbol{\Delta}\boldsymbol{V}^{\mathsf{H}} \\ \boldsymbol{O} \end{bmatrix}. \tag{4}$$

State variable conversion using matrix U The state variable conversion from $(\boldsymbol{A}, \boldsymbol{B}, \boldsymbol{C}, \boldsymbol{D})$ to $(\tilde{\boldsymbol{A}}, \tilde{\boldsymbol{B}}, \tilde{\boldsymbol{C}}, \tilde{\boldsymbol{D}})$ using the transformation matrix $\boldsymbol{U}^{\mathsf{H}}$ as $\tilde{\boldsymbol{x}}(s) = \boldsymbol{U}^{\mathsf{H}}\boldsymbol{x}(s)$ is given by

$$\tilde{\boldsymbol{A}} = \boldsymbol{U}^{\mathsf{H}}\boldsymbol{A}\boldsymbol{U}, \tag{5}$$
$$\tilde{\boldsymbol{B}} = \boldsymbol{U}^{\mathsf{H}}\boldsymbol{B} = \boldsymbol{\Sigma}\boldsymbol{V}^{\mathsf{H}} = \begin{bmatrix} \boldsymbol{\Delta}\boldsymbol{V}^{\mathsf{H}} \\ \boldsymbol{O}_{(n-m)\times m} \end{bmatrix}, \tag{6}$$
$$\tilde{\boldsymbol{C}} = \boldsymbol{C}\boldsymbol{U}, \tag{7}$$
$$\tilde{\boldsymbol{D}} = \boldsymbol{D} = \boldsymbol{O}_{m\times m}. \tag{8}$$

Zero Separation using system matrix The system matrix $\tilde{\boldsymbol{\Pi}}(s) \in \mathbb{R}^{(n+m)\times(n+m)}$ of $(\tilde{\boldsymbol{A}}, \tilde{\boldsymbol{B}}, \tilde{\boldsymbol{C}}, \tilde{\boldsymbol{D}})$ and $\tilde{\boldsymbol{W}}(s) \in \mathbb{R}^{n\times n}$ are represented as

$$\tilde{\boldsymbol{\Pi}}(s) = \left[\begin{array}{c|c} \tilde{\boldsymbol{A}} - s\boldsymbol{I} & \tilde{\boldsymbol{B}} \\ \hline \tilde{\boldsymbol{C}} & \tilde{\boldsymbol{D}} \end{array}\right], \tag{9}$$

$$\tilde{\boldsymbol{A}} - s\boldsymbol{I} = \tilde{\boldsymbol{W}}(s) = \begin{bmatrix} \tilde{\boldsymbol{W}}_u(s) \\ \tilde{\boldsymbol{W}}_l(s) \end{bmatrix}, \tag{10}$$

where $\tilde{\boldsymbol{W}}_u(s) \in \mathbb{C}^{m\times n}$, and $\tilde{\boldsymbol{W}}_l(s) \in \mathbb{C}^{(n-m)\times n}$.

The system $(\tilde{\boldsymbol{A}}, \tilde{\boldsymbol{B}}, \tilde{\boldsymbol{C}}, \tilde{\boldsymbol{D}})$ is represented by the system matrix $\tilde{\boldsymbol{\Pi}}(s)$ as follows:

$$\tilde{\boldsymbol{\Pi}}(s) \begin{bmatrix} \tilde{\boldsymbol{x}}(s) \\ \boldsymbol{u}(s) \end{bmatrix} = \begin{bmatrix} \boldsymbol{O}_{n\times m} \\ \boldsymbol{y}(s) \end{bmatrix}. \tag{11}$$

$\tilde{\boldsymbol{\Pi}}(s)$ is substituted each element as follows:

$$\left[\begin{array}{c|c} \tilde{\boldsymbol{W}}_u(s) & \boldsymbol{\Delta}\boldsymbol{V}^{\mathsf{H}} \\ \hline \tilde{\boldsymbol{W}}_l(s) & \boldsymbol{O}_{(n-m)\times m} \\ \hline \tilde{\boldsymbol{C}} & \boldsymbol{O}_{m\times m} \end{array}\right] \begin{bmatrix} \tilde{\boldsymbol{x}}(s) \\ \boldsymbol{u}(s) \end{bmatrix} = \begin{bmatrix} \boldsymbol{O}_{m\times m} \\ \boldsymbol{O}_{(n-m)\times m} \\ \boldsymbol{y}(s) \end{bmatrix}. \tag{12}$$

Since the system matrix $\tilde{\boldsymbol{\Pi}}(s)$ is a square matrix of $(n + m) \times (n + m)$, it is full rank if full row rank. The zeros of the system are defined as the values $s = z$ for which the polynomial system matrix $\tilde{\boldsymbol{\Pi}}(s)$ loses rank. When $\boldsymbol{\Delta}\boldsymbol{V}^{\mathsf{H}}$ is full rank, each line of the upper m rows is linearly independent with other lines for $\forall s$ because of the right side m columns. Therefore, the zeros of the system depend on the lower and left side $n \times n$ elements of the system matrix $\tilde{\boldsymbol{\Pi}}(s)$. Then, the lower and left side $n \times n$ elements of the system matrix are extracted as follows:

$$\begin{bmatrix} \tilde{\boldsymbol{W}}_l(s) \\ \tilde{\boldsymbol{C}} \end{bmatrix} \tilde{\boldsymbol{x}}(s) = \begin{bmatrix} \boldsymbol{O}_{(n-m)\times m} \\ \boldsymbol{y}(s) \end{bmatrix}. \tag{13}$$

Since multirate feedforward control solves the problems of unstable invariant zeros due to discretization, the problems of the continuous time unstable invariant zeros should be solved in the part of the state trajectory generation. Therefore, this state space realization is proposed for that the part of the state trajectory generation has all continuous time unstable invariant zero of the controlled system.

State trajectory generation The state trajectory $\tilde{\boldsymbol{x}}(s)$ from the output trajectory $\boldsymbol{y}(s)$ in the MIMO system is given by

$$\tilde{\boldsymbol{x}}(s) = \begin{bmatrix} \tilde{\boldsymbol{W}}_l(s) \\ \tilde{\boldsymbol{C}} \end{bmatrix}^{-1} \begin{bmatrix} \boldsymbol{O}_{(n-m)\times m} \\ \boldsymbol{y}(s) \end{bmatrix}. \tag{14}$$

From the state variable conversion using the transformation matrix $\boldsymbol{U}$ as $\boldsymbol{x}(s) = \boldsymbol{U}\tilde{\boldsymbol{x}}(s)$, the state trajectory $\boldsymbol{x}(s)$ from the output trajectory $\boldsymbol{y}(s)$ in the MIMO system is given by

$$\boldsymbol{U}\tilde{\boldsymbol{x}}(s) = \boldsymbol{U} \begin{bmatrix} \tilde{\boldsymbol{W}}_l(s) \\ \tilde{\boldsymbol{C}} \end{bmatrix}^{-1} \begin{bmatrix} \boldsymbol{O}_{(n-m)\times m} \\ \boldsymbol{y}(s) \end{bmatrix}$$
$$\Leftrightarrow \boldsymbol{x}(s) = \boldsymbol{U} \begin{bmatrix} \tilde{\boldsymbol{W}}_l(s) \\ \tilde{\boldsymbol{C}} \end{bmatrix}^{-1} \begin{bmatrix} \boldsymbol{O}_{(n-m)\times m} \\ \boldsymbol{y}(s) \end{bmatrix}. \tag{15}$$

By inverse Laplace transform, the desired state trajectory $\boldsymbol{x}_d(t)$ can be obtained from the desired output trajectory $\boldsymbol{y}_d(t)$ in the MIMO system:

$$\boldsymbol{x}_d(t) = \mathcal{L}^{-1}\left[\boldsymbol{U} \begin{bmatrix} \tilde{\boldsymbol{W}}_l(s) \\ \tilde{\boldsymbol{C}} \end{bmatrix}^{-1} \begin{bmatrix} \boldsymbol{O}_{(n-m)\times m} \\ \boldsymbol{y}_d(s) \end{bmatrix}\right]. \tag{16}$$

When the system has discretization unstable invariant zeros, the desired state trajectories become unstable because the inverse system which appears in the (16) has unstable poles. In this case, the convolution method with time axis reversal [Ohnishi et al. (2019)] is used and stable desired state trajectories with preactuation are generated. The preactuation means that control input occurs from negative time.

3. MULTIRATE FEEDFORWARD CONTROL FOR MULTI-INPUT MULTI-OUTPUT SYSTEM

Multirate feedforward control provides perfect tracking control [Fujimoto et al. (2001)]. A digital tracking control system typically has two samplers for the reference signal $r(t)$ and the output $y(t)$, and one holder on the input $u(t)$, as shown in Fig. 1. Therefore, three time periods exist: T_r, T_y, and T_u, which represent the periods of $r(t)$, $y(t)$, and $u(t)$, respectively. A larger T_r or T_y value is defined as the frame period T_f.

3.1 Definition of multi-input multi-output system

In an m-input p-output nth order MIMO system, the state equation (17) and the output equation (18) describing the continuous-time plant are given by

$$\dot{\boldsymbol{x}}(t) = \boldsymbol{A}_c\boldsymbol{x}(t) + \boldsymbol{B}_c\boldsymbol{u}(t), \tag{17}$$

$$\boldsymbol{y}(t) = \boldsymbol{C}_c\boldsymbol{x}(t), \tag{18}$$

$$\boldsymbol{B}_c = [\boldsymbol{b}_{c1}\ \cdots\ \boldsymbol{b}_{cm}], \quad \boldsymbol{C}_c = [\boldsymbol{c}_{c1}\ \cdots\ \boldsymbol{c}_{cp}]^{\mathsf{T}},$$

where the plant state is $\boldsymbol{x} \in \mathbb{R}^n$, the plant input is $\boldsymbol{u} \in \mathbb{R}^m$, and the plant output is $\boldsymbol{y} \in \mathbb{R}^p$.

3.2 Design of $\boldsymbol{B}$ matrix from generalized controllability indices

The generalized controllability indices are defined as follows [Fujimoto (2000)]:

Definition 1. (Generalized controllability indices). The generalized controllability indices of $(\boldsymbol{A}_c, \boldsymbol{B}_c)$ are defined below for $\boldsymbol{A}_c \in \mathbb{R}^{n\times n}$ and $\boldsymbol{B}_c = [\boldsymbol{b}_{c1}, \cdots, \boldsymbol{b}_{cm}] \in \mathbb{R}^{n\times m}$, respectively. If $(\boldsymbol{A}_c, \boldsymbol{B}_c)$ is a controllable pair, n linearly independent vectors including the linear combination can be selected from

$$\{\boldsymbol{b}_{c1}, \cdots, \boldsymbol{b}_{cm}, \boldsymbol{A}_c\boldsymbol{b}_{c1}, \cdots, \boldsymbol{A}_c\boldsymbol{b}_{cm}, \cdots, \boldsymbol{A}_c^{n-1}\boldsymbol{b}_{cm}\}.$$

The generalized controllability indices are the sets of the input multiplicities σ_l. The input multiplicities σ_l are defined as follows:

Definition 2. (Input multiplicities). Input multiplicities σ_l are defined as the number of the input which comes from the same input in the same frame period T_f.

Setting φ as a set of these n vectors, σ_l and N are defined by

$$\sigma_l = \text{number}\{k|\boldsymbol{A}_c^{k-1}\boldsymbol{b}_{cl} \in \varphi\}, \tag{19}$$

$$\sum_{l=1}^{m} \sigma_l = n, \tag{20}$$

$$N = \max(\sigma_l). \tag{21}$$

In the MIMO system, $n\,(=$ plant order$)$ vectors are selected from the generalized controllability indices, and the full row rank matrix $\boldsymbol{B}$ can be designed for almost all discretized sampling periods [1]. Therefore, feedforward controllers must be designed according to their different forms.

3.3 Feedforward input generation from state trajectory

From (22), the control inputs $\boldsymbol{u}_{ff}[i]$ required for PTC are given by (23).

$$\boldsymbol{x}[i+1] = \boldsymbol{A}\boldsymbol{x}[i] + \boldsymbol{B}\boldsymbol{u}[i], \tag{22}$$

$$\boldsymbol{u}_{ff}[i] = \boldsymbol{B}^{-1}(\boldsymbol{I} - z^{-1}\boldsymbol{A})\boldsymbol{x}[i+1], \tag{23}$$

where the matrices $\boldsymbol{A}$, $\boldsymbol{x}[i]$, $\boldsymbol{u}[i]$, z and T_f are given by

$$\boldsymbol{A} = e^{\boldsymbol{A}_c T_f}, \quad \boldsymbol{x}[i] = \boldsymbol{x}(iT_f), \quad z = e^{sT_f}, \quad T_f = NT_u,$$

$$\begin{aligned}\boldsymbol{u}[i] &= [\boldsymbol{u}_1[i]\ \cdots\ \boldsymbol{u}_m[i]]^{\mathsf{T}} \\ &= [u_{11}[i]\ \cdots\ u_{1\sigma_1}[i]\ u_{21}[i]\ \cdots\ u_{m\sigma_m}[i]]^{\mathsf{T}}.\end{aligned}$$

A block diagram of the control system is shown in Fig. 1. L is a discrete-time lifting operator [Chen and Francis (1995)]. L^{-1} outputs the elements of the nth dimensional vector $\boldsymbol{u}_{ff}[i]$, which is input at every period T_r, in the order from 1 to n by $T_u = T_r/n$.

3.4 Variety of MIMO multirate feedforward controllers

From these discussions, the multirate feedforward controllers for MIMO systems can be designed for several kinds depending on the selection of input multiplicities and they have different types of $\boldsymbol{B}$ matrix. It is confirmed that all designed controllers achieve perfect tracking control [Mae et al. (2018)]. Therefore, it is a problem that which controller design method is optimal for the controlled system. In the definition of perfect tracking control, the tracking error at the sampling point is only mentioned because the multirate feedforward controller is designed in the scheme of digital control. It is also necessary to reduce the tracking error between sampling points for the actual mechatronic applications. In this paper, we discuss the optimal method of selecting input multiplicities and constructing the $\boldsymbol{B}$ matrix for designing the optimal MIMO multirate feedforward controller.

4. SELECTION OF INPUT MULTIPLICITIES

When the multirate feedforward controller is designed with $\boldsymbol{B}$ chosen from the generalized controllability indices, the control input part of the state equation (22) is represented as follows:

$$\begin{aligned}&\boldsymbol{x}[i+1] = \boldsymbol{A}\boldsymbol{x}[i] + \boldsymbol{B}\boldsymbol{u}[i] \\ \Leftrightarrow\ &\boldsymbol{B}\boldsymbol{u}[i] = \boldsymbol{x}[i+1] - \boldsymbol{A}\boldsymbol{x}[i].\end{aligned} \tag{24}$$

The control input $\boldsymbol{u}[i]$ is represented by using the change of state trajectory $\boldsymbol{v}[i] = \boldsymbol{x}[i+1] - \boldsymbol{A}\boldsymbol{x}[i]$ as follows:

$$\begin{aligned}&\boldsymbol{B}\boldsymbol{u}[i] = \boldsymbol{v}[i] \\ \Leftrightarrow\ &\boldsymbol{u}[i] = \boldsymbol{B}^{-1}\boldsymbol{v}[i].\end{aligned} \tag{25}$$

[1] This is possible because the controllability of a continuous-time system is not preserved in the discrete system only if the two poles η_i and η_j have the same real parts, and the discretizing sampling period T satisfies $\eta_i = \eta_j + j\frac{2k\pi}{T}$ $(k = \pm1, \pm2, \ldots)$; furthermore, it is limited to only several cases.

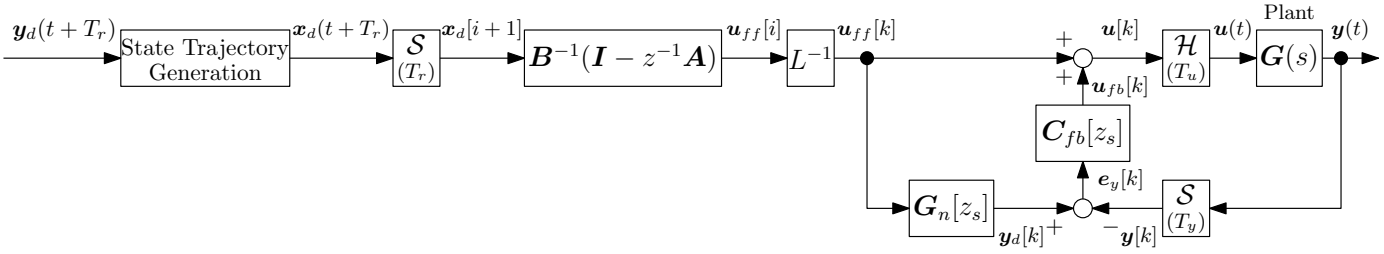

Fig. 1. Block diagram of controllers and a plant: a state trajectory generation, a multirate feedforward controller, and a singlerate feedback controller. $\mathcal{S}$, $\mathcal{H}$, and L denote a sampler, holder, and lifting operator [Chen and Francis (1995)], respectively, z and z_s denote e^{sT_r} and e^{sT_u}, respectively.

To evaluate the size of the control input, $||\boldsymbol{u}[i]||^2 = u_1^2 + \cdots + u_n^2$ is calculated as follows:

$$||\boldsymbol{u}[i]||^2 = \boldsymbol{v}^{\mathsf{T}}[i](\boldsymbol{B}^{-1})^{\mathsf{T}}\boldsymbol{B}^{-1}\boldsymbol{v}[i], \tag{26}$$

and $||\boldsymbol{u}[i]||^2$ becomes the quadratic form of $\boldsymbol{v}[i]$.

We define $||\boldsymbol{v}[i]||^2$ as 1 for considering the general desired state trajectory as follows:

$$||\boldsymbol{v}[i]||^2 = v_1^2 + \cdots + v_n^2 = 1. \tag{27}$$

When $||\boldsymbol{v}[i]||^2$ is 1, the range of $||\boldsymbol{u}[i]||^2$ is determined by the eigenvalue $\lambda_i((\boldsymbol{B}^{-1})^{\mathsf{T}}\boldsymbol{B}^{-1})$ as follows:

$$\lambda_n \le ||\boldsymbol{u}[i]||^2 \le \lambda_1 \quad (\lambda_n \le \lambda_{(n-1)} \le \cdots \le \lambda_1). \tag{28}$$

The eigenvalue $\lambda_{ci}(\boldsymbol{B}\boldsymbol{B}^{\mathsf{T}})$ has a relationship between the eigenvalue $\lambda_i((\boldsymbol{B}^{-1})^{\mathsf{T}}\boldsymbol{B}^{-1})$ as follows:

$$\lambda_{ci} = \frac{1}{\lambda_i}. \tag{29}$$

Then, the range of $||\boldsymbol{u}[i]||^2$ is determined by the eigenvalue $\lambda_{ci}(\boldsymbol{B}\boldsymbol{B}^{\mathsf{T}})$ as follows:

$$\frac{1}{\lambda_{cn}} \le ||\boldsymbol{u}[i]||^2 \le \frac{1}{\lambda_{c1}} \quad (\lambda_{c1} \le \lambda_{c2} \le \cdots \le \lambda_{cn}). \tag{30}$$

The singular value $\sigma_{ci}(\boldsymbol{B})$ has a relationship between the eigenvalue $\lambda_{ci}(\boldsymbol{B}\boldsymbol{B}^{\mathsf{T}})$ as follows:

$$\sigma_{ci}(\boldsymbol{B}) = \sqrt{\lambda_{ci}(\boldsymbol{B}\boldsymbol{B}^{\mathsf{T}})}. \tag{31}$$

Therefore, the range of the 2-norm of the control input $||\boldsymbol{u}[i]||_2$ is determined by the singular value $\sigma_{ci}(\boldsymbol{B})$ as follows:

$$\frac{1}{\sigma_{cn}} \le ||\boldsymbol{u}[i]||_2 \le \frac{1}{\sigma_{c1}} \quad (\sigma_{c1} \le \sigma_{c2} \le \cdots \le \sigma_{cn}). \tag{32}$$

When the 2-norm of control input is too large, it is not suitable for the mechatronic systems. Therefore, we design the optimal MIMO multirate feedforward controller from the viewpoint of the 2-norm of control input. To make the upper bound of the 2-norm of control input $||\boldsymbol{u}[i]||_2$ smaller, it is equal that the smallest singular value $\sigma_{c1}(\boldsymbol{B})$ makes larger. From this consideration, we should choose the input multiplicity so that the smallest singular value $\sigma_{c1}(\boldsymbol{B})$ is the largest.

5. SIMULATION

In the simulation, we verify the proposed guideline how to design the optimal MIMO multirate feedforward controller. We compare with the size of $\sigma_{c1}(\boldsymbol{B})$, the smallest singular value of $\boldsymbol{B}$, and the tracking errors in the simulation.

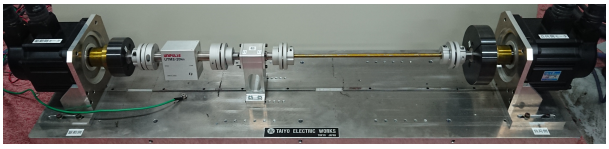

Fig. 2. Photograph of two inertia motor bench. In this paper, the two inertia motor bench is modeled as a two-input two-output system. The two inputs are motor side torque τ_m and load side torque τ_l, respectively. The two outputs are motor side angle θ_m and load side angle θ_l, respectively.

5.1 Plant model

In this simulation, we control the two-inertia motor bench system, shown in Fig. 2. The system is modeled as the two-input two-output fourth order plant model. The transfer function matrix $\boldsymbol{G}(s)$ of the plant is defined as (33). The inputs $\boldsymbol{u}(t) = [u_1(t)\ u_2(t)]^{\mathsf{T}} = [\tau_m(t)\ \tau_l(t)]^{\mathsf{T}}$ of the plant model are motor side torque τ_m and load side torque τ_l, respectively. The outputs $\boldsymbol{y}(t) = [y_1(t)\ y_2(t)]^{\mathsf{T}} = [\theta_m(t)\ \theta_l(t)]^{\mathsf{T}}$ of the plant model are motor side angle θ_m and load side angle θ_l, respectively. The plant model has coupling problem between each degree-of-freedom (DOF). In these MIMO coupled systems, MIMO multirate feedforward controller is needed to achieve perfect tracking control theoretically.

5.2 Controller design

We design several kinds of MIMO multirate feedforward controller depending on the selection of input multiplicities. Three sets of input multiplicities $(\sigma_1, \sigma_2) = (2,2), (3,1), (4,0)$ are used to design controllers. We design the matrix $\boldsymbol{B}$ from (34) to (36).

$\sigma_{c1}(\boldsymbol{B})$, the smallest singular value of $\boldsymbol{B}$, is compared with the simulation results in three kinds of controllers. $\sigma_{c1}(\boldsymbol{B})$ is calculated as Table 1. Considering from the size of $\sigma_{c1}(\boldsymbol{B})$, the sets of input multiplicity $(\sigma_1, \sigma_2) = (2,2)$ is the best to design MIMO multirate feedforward controller for this plant model $\boldsymbol{G}(s)$.

5.3 Conditions

The desired output trajectory $\boldsymbol{y}_d(t) = [y_{1d}(t)\ y_{2d}(t)]^{\mathsf{T}} = \left[\theta_m^{\mathrm{ref}}(t)\ \theta_l^{\mathrm{ref}}(t)\right]^{\mathsf{T}}$ is seventh-order polynomials. $\theta_m^{\mathrm{ref}}(t)$ is

$$\boldsymbol{G}(s) = \frac{1}{s^2(s^2+2.1\times10^5)}\begin{bmatrix} 9.7\times10^2(s^2+1.1\times10^5) & 1.1\times10^8 \\ 1.1\times10^8 & 1.1\times10^3(s^2+9.6\times10^4) \end{bmatrix} \tag{33}$$

$$(\sigma_1,\sigma_2) = (2,2) : \boldsymbol{B} = [\boldsymbol{A}_s\boldsymbol{b}_{s1}\ \ \boldsymbol{b}_{s1}\ \ \boldsymbol{A}_s\boldsymbol{b}_{s2}\ \ \boldsymbol{b}_{s2}] \tag{34}$$

$$(\sigma_1,\sigma_2) = (3,1) : \boldsymbol{B} = \left[\boldsymbol{A}_s^2\boldsymbol{b}_{s1}\ \ \boldsymbol{A}_s\boldsymbol{b}_{s1}\ \ \boldsymbol{b}_{s1}\ \ \boldsymbol{A}_s^2\boldsymbol{b}_{s2}+\boldsymbol{A}_s\boldsymbol{b}_{s2}+\boldsymbol{b}_{s2}\right] \tag{35}$$

$$(\sigma_1,\sigma_2) = (4,0) : \boldsymbol{B} = \left[\boldsymbol{A}_s^3\boldsymbol{b}_{s1}\ \ \boldsymbol{A}_s^2\boldsymbol{b}_{s1}\ \ \boldsymbol{A}_s\boldsymbol{b}_{s1}\ \ \boldsymbol{b}_{s1}\right] \tag{36}$$

from 0 to 100 µrad over a 0 to 0.1 s period. $\theta_l^{\mathrm{ref}}(t)$ is from 0 to 100 µrad over a 0 to 0.1 s period. $T_f = 12$ ms, $N = \max(\sigma_1,\sigma_2)$ and $T_f = NT_y = NT_u = T_r$. In this study, the actual plant $\boldsymbol{G}(s)$ and the nominal plant $\boldsymbol{G}_n(s)$ is the same. Therefore, the feedback controller $\boldsymbol{C}_{fb}[z_s]$ in Fig. 1 dose not work in the simulation.

If the experiment is conducted in actual mechatronic systems, a multirate feedforward controller is used with a feedback controller as a two-degree-of-freedom control system. A multirate feedforward controller handles the tracking performance and a feedback controller handles the rejection of the external disturbance and the modeling error.

5.4 Simulation results

The control inputs $\boldsymbol{u}(t) = [u_1(t)\ u_2(t)]^{\mathsf{T}} = [\tau_m(t)\ \tau_l(t)]^{\mathsf{T}}$ in the simulation are shown in Fig. 3. It is verified that, when the smallest singular value of $\boldsymbol{B}$ is large, the control inputs become small. The output $\boldsymbol{y}(t) = [y_1(t)\ y_2(t)]^{\mathsf{T}} = [\theta_m(t)\ \theta_l(t)]^{\mathsf{T}}$ in the simulation are shown in Fig. 4. The tracking errors become 0 at every sampling period T_f, demonstrating that perfect tracking control is achieved. Note that the values of the control input $\boldsymbol{u}$ and the output $\boldsymbol{y}$ in $(\sigma_1,\sigma_2) = (3,1)$ are too large compared with $(\sigma_1,\sigma_2) = (2,2),(4,0)$. Therefore, it can not be shown in detail in this range of plot due to the calculation error.

To evaluate the intersample behavior in the simulation, The root mean square and maximum absolute value of the control inputs $\boldsymbol{u}(t) = [u_1(t)\ u_2(t)]^{\mathsf{T}} = [\tau_m(t)\ \tau_l(t)]^{\mathsf{T}}$ and the tracking error $\boldsymbol{e}(t) = [e_1(t)\ e_2(t)]^{\mathsf{T}} = [e_{\theta_m}(t)\ e_{\theta_l}(t)]^{\mathsf{T}}$ are listed in Table 1. Compared with $\sigma_{c1}(\boldsymbol{B})$, the smallest singular value of $\boldsymbol{B}$, and the intersample behavior in the simulation results, it is verified that the sets of input multiplicity $(\sigma_1,\sigma_2) = (2,2)$ is the best to design MIMO multirate feedforward controller for this plant model $\boldsymbol{G}(s)$. The proposed method does not consider the specific cases of the desired trajectories, but the trend of the optimal controller can be evaluated by the proposed simple calculation method.

6. CONCLUSION

This paper proposes the guideline how to expand multirate feedforward control to the MIMO systems. Noteworthy, multirate feedforward control achieves perfect tracking control at every sampling point. In the actual mechatronic applications, however, intersample behavior is also a big issue for tracking control. We solve the problem due to unstable invariant zeros of the controlled system in the state trajectory generation and improve the intersample behavior. We also propose the guideline how to choose input multiplicities to design the optimal MIMO multirate feedforward controller from viewpoint of the 2-norm of control input.

The state space representation is calculated using the singular value decomposition of the $\boldsymbol{B}$ matrix. This representation gathers the continuous time unstable invariant zeros into a state trajectory generation part. The problem of the discrete time unstable invariant zeros is solved in a multirate feedforward control part. Therefore, the problem of continuous and discrete time unstable invariant zeros can be solved separately.

To design the optimal MIMO multirate feedforward controller, we focus on the 2-norm of control input. When 2-norm of control input is too large, it is not suitable for the mechatronic systems. We aim to make the 2-norm of control input smaller and the smaller control input also tend to the smaller tracking error between sampling points. It is an easier way compared with doing the simulation in all cases of the sets of input multiplicities. Using this method, the optimal MIMO multirate feedforward controller is designed which considers not only on tracking error at the sampling point but also intersample behavior. The effectiveness of the proposed method is verified in the simulation.

The proposed method evaluates the 2-norm of control input for the generalized desired state trajectory, but did not think about the relationship between the control input and the desired output trajectory in specific cases. The 2-norm of control input for the specific desired output trajectory also can be calculated. An analysis of the relationship between the plant and the desired output trajectories, the experimental validation and considering mechatronic constraints are future research.

REFERENCES

Butler, H. (2011). Position Control in Lithographic Equipment [Applications of Control]. *IEEE Control Systems*, 31(5), 28–47. doi:10.1109/MCS.2011.941882.

Butterworth, J., Pao, L., and Abramovitch, D. (2012). Analysis and comparison of three discrete-time feedforward model-inverse control techniques for nonminimum-phase systems. *Mechatronics*, 22(5), 577–587. doi:10.1016/j.mechatronics.2011.12.006.

Chen, T. and Francis, B.A. (1995). *Optimal Sampled-Data Control Systems*. Springer London, London. doi:10.1007/978-1-4471-3037-6.

Fujimoto, H. (2000). General Framework of Multirate Sampling Control and Applications to Motion Control Systems. *Doctoral Dissertation*.

Fujimoto, H., Hori, Y., and Kawamura, A. (2001). Perfect tracking control based on multirate feedforward control with generalized sampling periods. *IEEE Transactions*

Table 1. $\sigma_{c1}(\boldsymbol{B})$, the smallest singular value of $\boldsymbol{B}$, and root mean square and maximum absolute value of control inputs $\boldsymbol{u}$ and tracking errors $\boldsymbol{e}$ depending on sets of input multiplicities (σ_1, σ_2).

(σ_1, σ_2)	$\sigma_{c1}(\boldsymbol{B})$	RMS(u_1)	MAX($\lvert u_1 \rvert$)	RMS(u_2)	MAX($\lvert u_2 \rvert$)	RMS(e_1)	MAX($\lvert e_1 \rvert$)	RMS(e_2)	MAX($\lvert e_2 \rvert$)
$(2, 2)$	3.17×10^{-5}	5.24×10^{-5}	7.76×10^{-5}	4.42×10^{-5}	6.56×10^{-5}	1.45×10^{-8}	3.44×10^{-8}	1.45×10^{-8}	3.44×10^{-8}
$(3, 1)$	1.84×10^{-14}	2.22×10^{4}	4.11×10^{4}	1.91×10^{4}	2.90×10^{4}	1.38×10^{2}	3.54×10^{2}	1.01×10^{2}	2.52×10^{2}
$(4, 0)$	5.28×10^{-6}	1.22×10^{-4}	1.98×10^{-4}	0	0	3.47×10^{-7}	7.71×10^{-7}	2.18×10^{-7}	5.07×10^{-7}

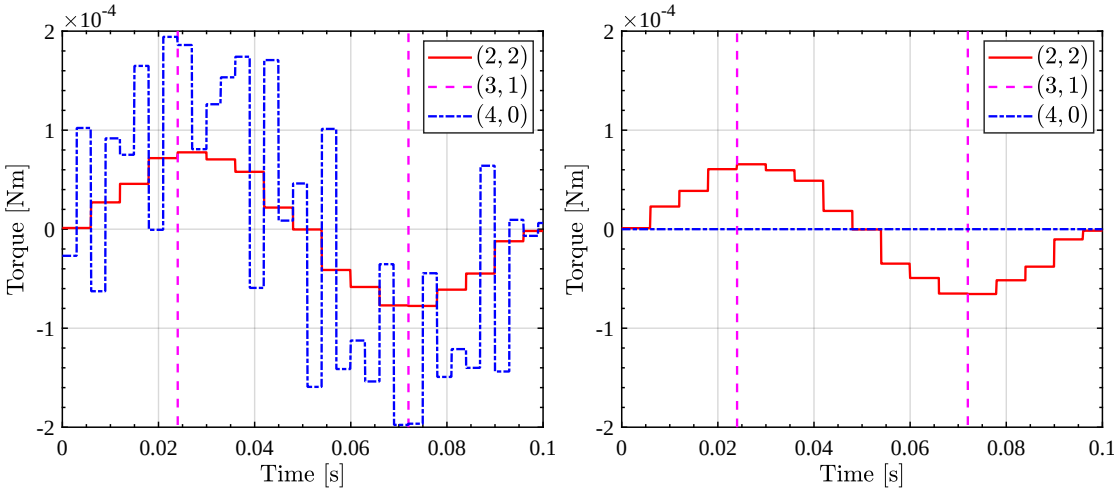

(a) τ_m (b) τ_l

Fig. 3. Control Input $\boldsymbol{u}$: Control Input of $(\sigma_1, \sigma_2) = (2, 2)$ and $(4, 0)$ is not so large, but, that of $(\sigma_1, \sigma_2) = (3, 1)$ is too large and is not suitable for the mechatronic systems.

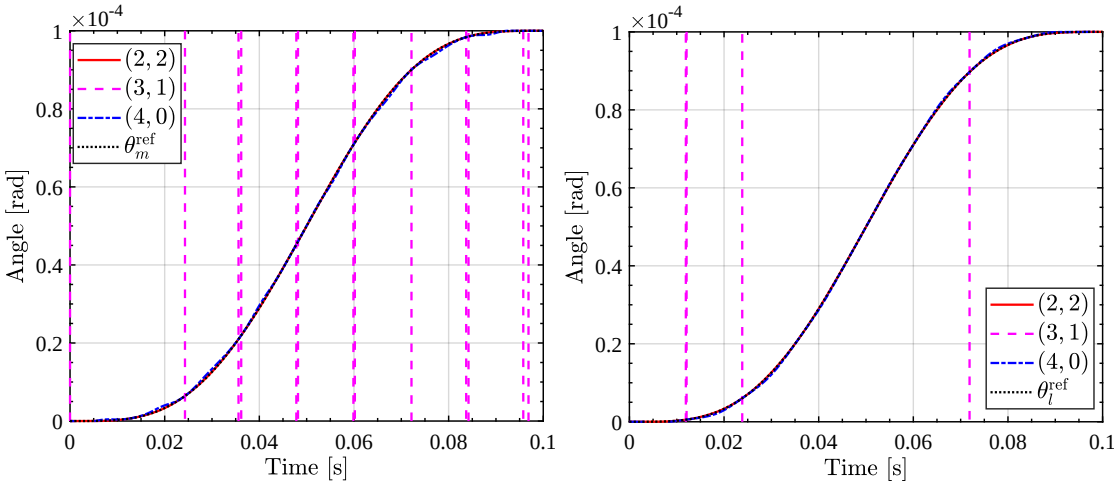

(a) θ_m (b) θ_l

Fig. 4. Output $\boldsymbol{y}$: perfect tracking control is achieved and tracking errors at every sampling points become zero for the nominal plant, theoretically. However, the intersample behavior is different depending on the sets of the input multiplicities $(\sigma_1, \sigma_2) = (2, 2), (3, 1)$ and $(4, 0)$.

on Industrial Electronics, 48(3), 636–644. doi:10.1109/41.925591.

Mae, M., Ohnishi, W., Fujimoto, H., and Hori, Y. (2018). Perfect Tracking Control of Dual-Input Dual-Output System for High-Precision Stage in Translation and Pitching Motion. *Proceedings of the International Workshop on Sensing, Actuation, Motion Control, and Optimization*, (5), TT6–5.

Ohnishi, W., Beauduin, T., and Fujimoto, H. (2019). Preactuated Multirate Feedforward Control for Independent Stable Inversion of Unstable Intrinsic and Discretization Zeros. *IEEE/ASME Transactions on Mechatronics*. doi:10.1109/TMECH.2019.2896237.

Tomizuka, M. (1987). Zero Phase Error Tracking Algorithm for Digital Control. *Journal of Dynamic Systems, Measurement, and Control*, 109(1), 65. doi:10.1115/1.3143822.

Wen, J. and Potsaid, B. (2004). An experimental study of a high performance motion control system. In *Proceedings of the 2004 American Control Conference*, volume 6, 5158–5163. IEEE. doi:10.23919/ACC.2004.1384671.